Interplay between Water and TiO_2 Anatase (101) Surface with Subsurface Oxygen Vacancy

Yadong Li[1,2] and Yi Gao[1,*]

[1]Division of Interfacial Water and Key Laboratory of Interfacial Physics and Technology, Shanghai Institute of Applied Physics, Chinese Academy of Sciences, Shanghai 201800, China

[2]University of Chinese Academy of Sciences, Beijing 100049, China

(Received 7 November 2013; revised manuscript received 18 February 2014; published 20 May 2014)

The interaction between water and the TiO_2 anatase (101) surface with a subsurface V_O is studied using first-principles calculations. Upon water adsorption, the relative stability of the subsurface and surface V_O reverses. The surface V_O becomes energetically more stable than its subsurface counterpart, which induces V_O to migrate from the subsurface to the surface with a very low energy barrier. Then the adsorbed water molecule can easily dissociate through a barrierless pathway facilitated by surface V_O. This reaction pathway has a similar energy barrier with another pathway under which water dissociates with the presence of subsurface V_O followed by V_O migration from the subsurface layer to the surface layer, indicating that subsurface V_O can facilitate water dissociation directly, or, via surface V_O indirectly. This novel interplay between the adsorbate and substrate defects may provide a new way to explain the origin of the activity of anatase (101) in photocatalysis in aqueous surroundings.

DOI: 10.1103/PhysRevLett.112.206101 PACS numbers: 68.47.Gh, 68.35.B-, 68.43.-h

TiO_2 is an inexpensive, nontoxic, metal oxide with applications in a wide range of areas, such as photocatalysis and self-cleaning materials [1,2]. The adsorption and dissociation of water on TiO_2 surfaces have brought a particular intensive research interest because it is the preliminary step for water-splitting [1] and water-gas shift reactions [3]. Besides TiO_2 rutile [4], TiO_2 anatase only attracted scientists' research interests in recent years due to the difficulty in obtaining a large size anatase crystal [5]. When the particle size is less than 11 nm [4], anatase is the most stable TiO_2 phase among brookite, anatase, and rutile—the three most common TiO_2 phases—and is believed to be catalytically more active than rutile [6]. The (101) surface is the predominant anatase surface due to its lower surface energy compared with other minor surfaces [e.g., the (001) or (100) surface]. Thereby, a full understanding of the interplay between the predominant (101) surface and water molecules is crucial for further study of the reactivity of anatase nanoparticles.

Water adsorption on the stoichiometric anatase (101) surface has been studied since the 1990s. Molecular adsorption has been confirmed to be energetically more favorable than dissociative adsorption by experimental and theoretical methods [5,7]. It is known that surface defects can affect a material's activity substantially by exposing low-coordinated surface atoms [8]. For example, with the combination of experimental and theoretical efforts, the abundant surface oxygen vacancies (V_O^{sur}'s) on the TiO_2 rutile (110) surface have been proved unambiguously to be the active sites for water dissociation [8,9]. In contrast with rutile, V_O's on the anatase (101) surface are unstable. Because of the difficulty of forming V_O^{sur}'s, there are only scattered experiments about O_2 and formic acid interacting with a defective anatase (101) surface [10–12]. While for water adsorption a recent study based on diffuse reflectance infrared Fourier transform spectroscopy (DRIFTS) suggests dissociation of water on a defective anatase (101) surface [13]. And, there is overwhelming theoretical evidence that shows water can dissociate over the V_O^{sur}'s or several types of steps [14–16]. Interestingly, a recent scanning tunneling microscopy (STM) study by He *et al.* found V_O's are predominant on the subsurface region of anatase (101) [17]. The following theoretical and experimental studies confirmed that subsurface oxygen vacancies (V_O^{sub}'s) are energetically more stable than V_O^{sur}'s, and V_O migration barriers from the surface layer to the subsurface layer range from 0.6 to 1.2 eV, depending on the immediate environment [18,19]. For water adsorption on the surface with V_O^{sub}, density-functional theory (DFT) calculations showed that molecular adsorption configuration remains energetically more stable than the dissociative one, with enhanced adsorption strength comparing to the stoichiometric surface, and a facile dissociation pathway with energy barrier of 0.26 eV was also identified [20], which is still waiting for experimental confirmation.

The relative stability of surface and subsurface V_O could be reversed with the adsorption of small molecules on the surface. Setvín *et al.* first discovered an extraordinary interaction between O_2 and V_O^{sub} on TiO_2 anatase (101) with joint experimental and theoretical efforts [11]. Their results showed that the V_O^{sub} migrates to surface upon O_2 adsorption, and then induces O_2 to form a bridging $(O_2)_O$ species via a low barrier of 47 meV. Considering the

importance of $(O_2)_O$ as the intermediate in the photooxidation of water [21], this interaction "could contribute to the higher photocatalytic activity of anatase relative to rutile" [21]. Besides O_2, the adsorption of perylene with a carboxylic acid anchor group could also reverse the relative stability between $V_O{}^{sur}$ and $V_O{}^{sub}$ to make $V_O{}^{sub}$ no longer prevail [22].

In this Letter, the novel interplays between water and TiO_2 anatase (101) with $V_O{}^{sub}$ are proposed theoretically. The adsorption of the water molecule on the surface with $V_O{}^{sub}$ decreases its relative stability compared to the surface with $V_O{}^{sur}$, which induces $V_O{}^{sub}$ to bubble up to the surface to become $V_O{}^{sur}$ with a low energy barrier. Then $V_O{}^{sur}$, in turn, facilitates the dissociation of the water molecule through a barrierless pathway, forming two bridging hydroxyl groups along the $[11\bar{1}]$ direction. To our knowledge, this novel interplay between water and substrate has not been reported previously. Meanwhile, another energetically competitive pathway of water dissociation with the presence of $V_O{}^{sub}$ followed by V_O migration from the subsurface layer to the surface layer is also presented. These findings may provide an alternative explanation of the activity of the anatase (101) surface in photocatalysis in aqueous surroundings and enrich our knowledge about molecule adsorption on the metal oxide surface.

Calculations are carried out using spin-polarized DFT with the generalized gradient approximation (GGA) of Perdew-Burke-Ernzerhof (PBE) implemented in the VASP code [23–25]. Starting with a lattice parameter of $a = 3.73$ and $c = 9.37$ Å [26], we obtained $a = 3.78$ and $c = 9.45$ Å after full relaxation of the unit cell. A model structure with three O-Ti-O layers is used to simulate the TiO_2 anatase (101) surface. The bottom layer is fixed to mimic the bulk structure. A$(1 * 4)$ supercell with 144 atoms exposes a surface area of $10.18 * \times 15.13$ Å^2. A vacuum layer of 20 Å is used to exclude the influence of vertical periodic images. Because of the large supercell, k-point sampling is restricted to the Γ point. The interaction between core and valence electrons is described by projector augmented wave method with an energy cutoff of 400 eV [27,28]. The $3s$, $3p$, $3d$, and $4s$ electrons of Ti and the $2s$, $2p$ electrons of O are considered as valence electrons explicitly. For DFT + U calculations, the on-site Coulomb repulsion parameter U for the Ti $3d$ orbital is set to be 3.5 eV, consistent with previous literature [10,11]. The nudged elastic band method is used for the transition state calculations [29].

Formation energy of $V_O{}^{sub}/V_O{}^{sur}$ and water adsorption energy on stoichiometric surfaces are calculated to validate the accuracy of our results. Our calculation shows V_O formation energy in the subsurface layer is lower than that in the surface layer. The V_O formation energy is 4.18 eV for V_O1 (most stable surface vacancy, see Fig. 1) at the surface layer and 4.00 eV for V_O4 at the subsurface layer, quantitatively consistent with the previous calculation (4.25 and 4.03 eV, respectively) [18]. The V_Ox configuration is unstable and will relax to the V_O1 configuration after geometry optimization. All V_O formation energies are listed in Table I. The water monomer adsorbs on the stoichiometric surface exothermally with a binding energy of −0.79 eV, consistent with the previous results of −0.73 [5] and −0.72 eV [20].

TABLE I. Surface and subsurface V_O formation energies.

V_O	Formation energy (eV)
V_O1	4.18
V_O2	4.89
V_O3	4.54
V_O4	4.00

The eight surface Ti − 5c (five-coordinated Ti) atoms are equivalent sites for water adsorption on the stoichiometric $(1 * 4)$ surface supercell. But with the introduction of $V_O{}^{sub}$, five distinct adsorption sites emerge due to their relative positions to the subsurface defect (see Fig. S1 [30]). $V_O{}^{sub}$'s second nearest neighboring Ti − 5c (S5 in Fig. S1 [30]) is most stable for water adsorption with a binding energy of −0.84 eV. The adsorption configuration is illustrated in Fig. 2(c), denoted as M^{sub}. For adsorption energies of the rest of the adsorption sites, please refer to Table SI [30].

The water adsorption of the surface with $V_O{}^{sur}$ is much stronger than that of the surface with $V_O{}^{sub}$. Ti − 4c and Ti − 5c in the vicinity of the surface defect have been thoroughly examined as possible adsorption sites. The Ti − 4c near $V_O{}^{sur}$ [$M_1{}^{sur}$ in Fig. 2(d)] is the most favorable adsorption site with a binding energy of −1.20 eV. Adsorption of water induces substantial structural relaxation. The oxygen atom just below $V_O{}^{sur}$ moves upwards

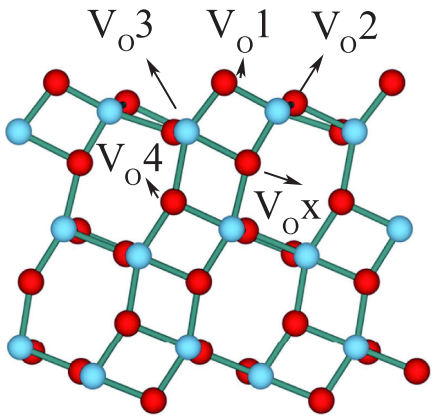

FIG. 1 (color online). Side view of the three-layer TiO_2 anatase (101) surface. Five different V_O sites (numbered from V_O1 to V_O4, and V_Ox) are also shown. Ti atoms are represented by blue (light gray) spheres; O atoms are represented by red (dark gray) spheres.

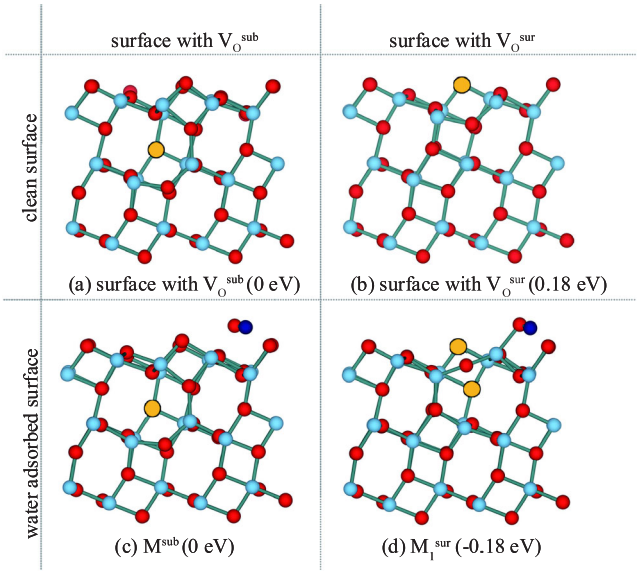

FIG. 2 (color online). Structures of the surface with V_O^{sub}, V_O^{sur} and their relative energies are shown in (a) and (b), respectively. Structures of water adsorbed on the surface with V_O^{sub}, V_O^{sur} and their relative energies are shown in (c) and (d), respectively. H atoms are represented by dark blue (black) spheres; Ti atoms are represented by blue (light gray) spheres; O atoms are represented by red (dark gray) spheres; V_O's are represented by yellow (white) spheres.

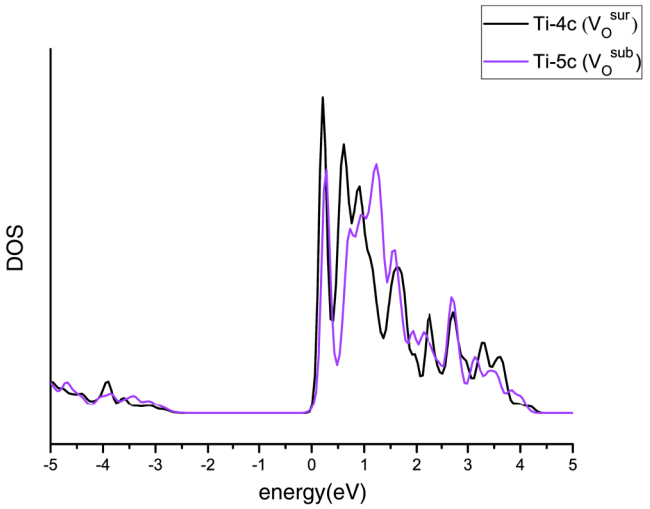

FIG. 3 (color online). Projected density of states (DOS) of the clean surface's Ti atom where water will be adsorbed on. The DOS are aligned with their respective Fermi levels.

substantially, breaking the $Ti-O$ bond with the second layer Ti atom.

Dissociative adsorption configuration is more stable than molecular adsorption configuration on the surface with V_O^{sur}. The two most stable adsorption configurations, D_1^{sur} [Fig. S2(d)] and D_2^{sur} [Fig. S4(d)] [30], are identified with adsorption energy of -1.77 and -1.82 eV, respectively. The D_1^{sur} configuration is energetically more favorable than the M_1^{sur} configuration by 0.57 eV. These results are consistent with the previous results by Tilocca and Selloni [15].

For clean anatase (101), V_O^{sub} is energetically more stable than V_O^{sur} by about 0.18 eV. But the water adsorption energy of the M_1^{sur} configuration is 0.36 eV more negative than that of the M^{sub} configuration. This can be rationalized by the shorter $O-H_W$ (hydrogen atom from water) and $Ti-O_W$ (oxygen atom from water) bond distances of M_1^{sur} ($Ti-O_W$: 2.14 Å; $O-H_W$: 1.85 Å) comparing with M^{sub} ($Ti-O_W$: 2.21 Å; $O-H_W$: 1.99 Å). On the other hand, the stronger H_2O adsorption of V_O^{sur} over V_O^{sub} could also be explained by a stronger $3d$ peak of $Ti-4c$ on surface with V_O^{sur} at the conduction band minimum compared to that of $Ti-5c$ on surface with V_O^{sub} (Fig. 3), and the larger downward shift of the d-band center of the surface with V_O^{sur} compared to that of the surface with V_O^{sub} (0.05 vs 0.04 eV). Thus, the relative stability of V_O^{sub} and V_O^{sur} is reversed after water adsorption. The surface with V_O^{sur} is 0.18 eV lower in energy than the surface with V_O^{sub} with water adsorption. Considering that the D_1^{sur} dissociative configuration is energetically more stable, we expect that V_O may migrate from the subsurface layer to the surface layer, and induce the adsorbed water dissociate to form two hydroxyl groups on the surface. The following transition state calculations confirmed our speculation.

The calculated V_O migration pathway and atomic configurations are shown in Fig. 4. Initially, the water molecule comes close to the anatase (101) surface and adsorbs on the strongest adsorption site (S5 in Fig. S1 [30]) over V_O^{sub} with binding energy of -0.84 eV. Upon water adsorption, the relative stability of V_O^{sub} decreases and the surface reconstruction happens. By crossing a 0.09 eV energy barrier, the oxygen atom just below the surface $O-2c$ (two-coordinated oxygen) moves towards the subsurface defect site, breaking the $Ti-O$ bond with the first layer Ti atom. Meanwhile, the surface Ti atom moves upward, forming a stronger bond with the water molecule. The $Ti-O_W$ and $O-H_W$ bond lengths reduce to 2.05 and 1.74 Å, respectively. Then the surface oxygen atom migrates to the subsurface defect site, leaving V_O on the surface layer. The V_O migration is followed by barrierless water dissociation with the presence V_O^{sur}, as shown in Fig. S2 [30]. It is clear H_W readily dissociates from water and migrates to its neighboring $O-2c$ atom. Then the OH group lies down to fill V_O^{sur}. The final state (D_1^{sur}) is characterized by two bridging OH groups along the $[11\bar{1}]$ direction.

We have also identified another energetically competitive pathway of water dissociation over V_O^{sub} (Fig. S5 [30]) followed by V_O^{sub} migration to the surface (Fig. 5). Water dissociates over V_O^{sub} after crossing a 0.12 eV energy barrier. The dissociative water induces substantial structural relaxation [Fig. 5(a)] and V_O migration to the surface layer via a barrierless pathway. Figure 5(c) shows a metastable

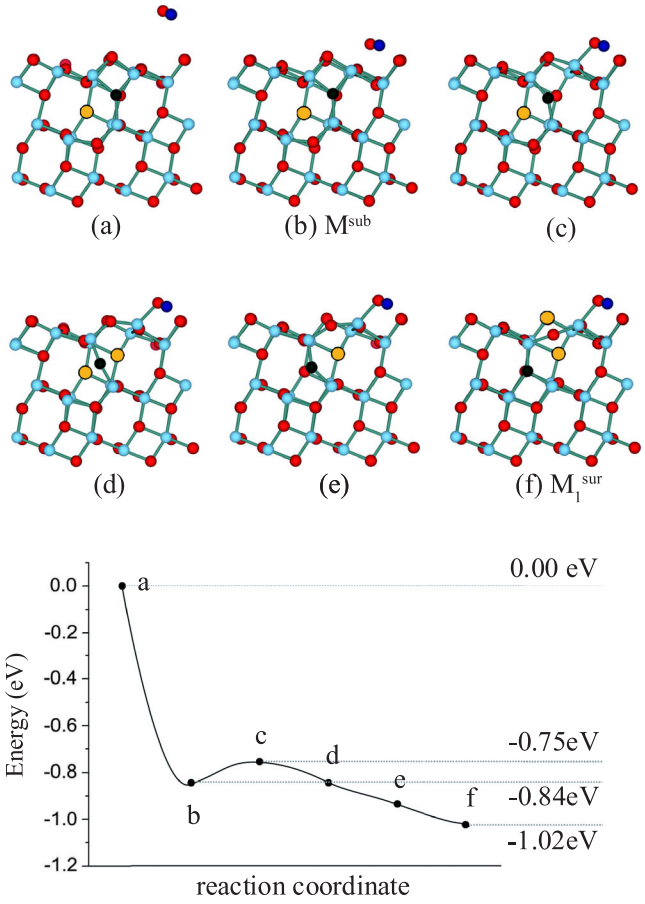

FIG. 4 (color online). Selected atomic configurations along the pathway for V_O migration from the subsurface to the surface with water molecularly adsorbed on the surface. H atoms are represented by dark blue (black) spheres; Ti atoms are represented by blue (light gray) spheres; O atoms are represented by red (dark gray) spheres; V_O's are represented by yellow (white) spheres with black edges; O atoms with larger displacement are represented in dark green (black) spheres.

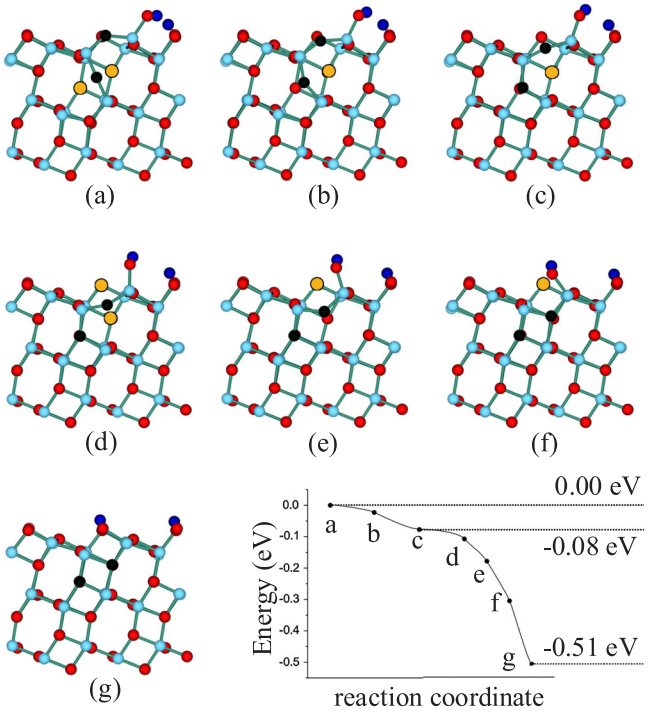

FIG. 5 (color online). Selected atomic configurations along the pathway for V_O migration from the subsurface to the surface with water dissociatively adsorbed on the surface. H atoms are represented by dark blue (black) spheres; Ti atoms are represented by blue (light gray) spheres; O atoms are represented by red (dark gray) spheres; V_O's are represented by yellow (white) spheres with black edges; O atoms with larger displacement are represented in dark green (black) spheres. For Fig. 5(g), the periodic image of H adsorbed on $O-2c$ at the left side of the image is removed for clarity.

state structurally similar to Fig. S2(b) of [30]. The dangling OH group adsorbed on the lattice Ti atom may participate in other reactions with introduction of a reactant [13].

To verify the accuracy of the GGA results, GGA + U calculations are also performed [10,11]. The adsorption energy of the water molecule over V_O^{sub} is −0.90 eV, less stable than over V_O^{sur} by 0.07 eV. For the surface with V_O^{sub}, another energy-degenerate adsorption configuration (with one hydrogen bond between water and the surface) is identified with a binding energy of −0.93 eV (see Fig. S6 [30] for comparison with M^{sub}), consistent with previous results [20]. Here, only M^{sub} (with two hydrogen bonds between water and the surface) is considered in the transition state calculation as a comparison with the GGA results. The migration barrier from V_O^{sub} to V_O^{sur} with molecular water adsorption is 0.15 eV. Then the adsorbed water dissociates barrierlessly, consist with GGA results. For another competitive pathway, water dissociates with V_O residing on the subsurface layer by overcoming the 0.13 eV barrier. Then the V_O^{sub} can readily migrate to the surface layer barrierlessly, similar to the result from GGA calculations. These results, together with previous calculations, show the GGA is reliable to describe the interaction between water and the reduced anatase surface [20,31].

In summary, by utilizing DFT calculation, we find a novel interplay between adsorbed water and subsurface V_O. With H_2O adsorption, V_O^{sur} becomes more stable than V_O^{sub} and can easily induce V_O^{sub} to migrate to the surface layer, which further facilitates H_2O dissociation. In the meantime, another mechanism for water dissociation is also feasible. Molecular water dissociates with the presence of V_O^{sub} first, followed by V_O^{sub} migration to the surface layer. Both pathways have similar activation energy barriers, which indicate the adsorption of the water molecule on the surface with V_O^{sub} may undergo either pathways with similar possibility; in other words, V_O^{sub} can facilitate water dissociation directly or via V_O^{sur} indirectly. Considering that ample experimental evidence suggests V_O^{sur} is photocatalytically more active than V_O^{sub} [32–34],

our finding may provide an alternative way to understand the catalytic activity of anatase (101) in aqueous surroundings [35]. The catalytic activity of the anatase (101) surface not only explicitly depends on the density of V_O^{sur}, but also inexplicitly depends on the density of total V_O. As subsurface vacancies widely present on other systems (e.g., CeO_2) [36], our results may also apply to these systems. Whether other molecule adsorption, for example, hydrogen or organic molecules, will introduce such V_O migration is waiting for further study.

We thank Professor Hai-Ping Fang for discussion. This work is supported by the startup funding from the Shanghai Institute of Applied Physics, Chinese Academy of Sciences (Y290011011), National Natural Science Foundation of China (21273268), "Hundred People Project" from the Chinese Academy of Sciences, and "Pu-jiang Rencai Project" from the Science and Technology Commission of Shanghai Municipality (13PJ1410400). The computational resources utilized in this research were provided by the Shanghai Supercomputer Center, the National Supercomputing Center in Tianjin, and the Supercomputing Center of the Chinese Academy of Sciences in Beijing.

*gaoyi@sinap.ac.cn

[1] A. Fujishima and K. Honda, Nature (London) **238**, 37 (1972).
[2] R. Wang, K. Hashimoto, A. Fujishima, M. Chikuni, E. Kojima, A. Kitamura, M. Shimohigoshi, and T. Watanabe, Nature (London) **388**, 431 (1997).
[3] J. A. Rodriguez, S. Ma, P. Liu, J. Hrbek, J. Evans, and M. Pérez, Science **318**, 1757 (2007).
[4] H. Zhang and J. F. Banfield, J. Phys. Chem. B **104**, 3481 (2000).
[5] Y. He, A. Tilocca, O. Dulub, A. Selloni, and U. Diebold, Nat. Mater. **8**, 585 (2009).
[6] L. Kavan, M. Grätzel, S. E. Gilbert, C. Klemenz, and H. J. Scheel, J. Am. Chem. Soc. **118**, 6716 (1996).
[7] A. Vittadini, A. Selloni, F. P. Rotzinger, and M. Grätzel, Phys. Rev. Lett. **81**, 2954 (1998).
[8] O. Bikondoa, C. L. Pang, R. Ithnin, C. A. Muryn, H. Onishi, and G. Thornton, Nat. Mater. **5**, 189 (2006).
[9] R. Schaub, P. Thostrup, N. Lopez, E. Lægsgaard, I. Stensgaard, J. K. Nørskov, and F. Besenbacher, Phys. Rev. Lett. **87**, 266104 (2001).
[10] H. Cheng and A. Selloni, J. Chem. Phys. **131**, 054703 (2009).
[11] M. Setvín, U. Aschauer, P. Scheiber, Y.-F. Li, W. Hou, M. Schmid, A. Selloni, and U. Diebold, Science **341**, 988 (2013).
[12] M. Xu, H. Noei, M. Buchholz, M. Muhler, C. Wöll, and Y. Wang, Catal. Today **182**, 12 (2012).
[13] L. Liu, H. Zhao, J. M. Andino, and Y. Li, ACS Catal. **2**, 1817 (2012).
[14] A. Tilocca and A. Selloni, J. Phys. Chem. B **108**, 4743 (2004).
[15] A. Tilocca and A. Selloni, J. Chem. Phys. **119**, 7445 (2003).
[16] X. Q. Gong, A. Selloni, M. Batzill, and U. Diebold, Nat. Mater. **5**, 665 (2006).
[17] Y. He, O. Dulub, H. Cheng, A. Selloni, and U. Diebold, Phys. Rev. Lett. **102**, 106105 (2009).
[18] H. Cheng and A. Selloni, Phys. Rev. B **79**, 092101 (2009).
[19] P. Scheiber, M. Fidler, O. Dulub, M. Schmid, U. Diebold, W. Hou, U. Aschauer, and A. Selloni, Phys. Rev. Lett. **109**, 136103 (2012).
[20] U. Aschauer, Y. He, H. Cheng, S.-C. Li, U. Diebold, and A. Selloni, J. Phys. Chem. C **114**, 1278 (2010).
[21] Y.-F. Li, Z.-P. Liu, L. Liu, and W. Gao, J. Am. Chem. Soc. **132**, 13 008 (2010).
[22] S. Ikalainen and K. Laasonen, Phys. Chem. Chem. Phys. **15**, 11 673 (2013).
[23] J. P. Perdew, K. Burke, and M. Ernzerhof, Phys. Rev. Lett. **77**, 3865 (1996).
[24] G. Kresse and J. Furthmüller, Phys. Rev. B **54**, 11169 (1996).
[25] G. Kresse and J. Furthmüller, Comput. Mater. Sci. **6**, 15 (1996).
[26] U. Diebold, Surf. Sci. Rep. **48**, 53 (2003).
[27] P. E. Blöchl, Phys. Rev. B **50**, 17953 (1994).
[28] G. Kresse and D. Joubert, Phys. Rev. B **59**, 1758 (1999).
[29] G. Henkelman, B. P. Uberuaga, and H. Jonsson, J. Chem. Phys. **113**, 9901 (2000).
[30] See Supplemental Material at http://link.aps.org/supplemental/10.1103/PhysRevLett.112.206101 for more detailed information.
[31] A. Tilocca and A. Selloni, J. Phys. Chem. C **116**, 9114 (2012).
[32] J. Yan, G. Wu, N. Guan, L. Li, Z. Li, and X. Cao, Phys. Chem. Chem. Phys. **15**, 10 978 (2013).
[33] X. Yu, B. Kim, and Y. K. Kim, ACS Catal. **3**, 2479 (2013).
[34] M. Kong, Y. Li, X. Chen, T. Tian, P. Fang, F. Zheng, and X. Zhao, J. Am. Chem. Soc. **133**, 16 414 (2011).
[35] J. Pan, G. Liu, G. Q. Lu, and H.-M. Cheng, Angew. Chem., Int. Ed. **50**, 2133 (2011).
[36] M. V. Ganduglia-Pirovano, J. L. F. Da Silva, and J. Sauer, Phys. Rev. Lett. **102**, 026101 (2009).